

Lyapunov Neural ODE Feedback Control Policies

Joshua Hang Sai Ip, Georgios Makrygiorgos, Ali Mesbah

Abstract—Deep neural networks are increasingly used as an effective way to represent control policies in a wide-range of learning-based control methods. For continuous-time optimal control problems (OCPs), which are central to many decision-making tasks, control policy learning can be cast as a neural ordinary differential equation (NODE) problem wherein state and control constraints are naturally accommodated. This paper presents a Lyapunov-NODE control (L-NODEC) approach to solving continuous-time OCPs for the case of stabilizing a known constrained nonlinear system around a terminal equilibrium point. We propose a Lyapunov loss formulation that incorporates a control-theoretic Lyapunov condition into the problem of learning a state-feedback neural control policy. We establish that L-NODEC ensures exponential stability of the controlled system, as well as its adversarial robustness to uncertain initial conditions. The performance of L-NODEC is illustrated on a benchmark double integrator problem and for optimal control of thermal dose delivery using a cold atmospheric plasma biomedical system. L-NODEC can substantially reduce the inference time necessary to reach the equilibrium state.

I. INTRODUCTION

Optimal control is foundational to decision-making for complex dynamical systems [1], [2]. Efficient solution methods for optimal control problems (OCPs) are essential for tasks such as optimization-based parameter and state estimation, optimal experimental design, and model-based control [3]. Solving continuous-time OCPs is generally challenging, especially for systems with nonlinear dynamics and path constraints, since these OCPs involve infinitely many decision variables in the form of time-varying functions. Various optimization techniques are developed to solve continuous-time OCPs, including direct methods that approximate the original infinite-dimensional problem as a finite-dimensional one via discretization of the time-varying functions [4], [5], indirect methods that look to solve the necessary conditions of optimality using Pontryagin’s maximum principle or the Hamilton–Jacobi–Bellman equation [6], [7], and global optimization methods [8], [9].

In this work, we adopt a learning perspective to solving continuous-time OCPs. In particular, (deep) neural networks (NN) are widely used to represent control policies in reinforcement learning (RL) for Markov decision processes [10],

which fundamentally relies on optimal control [11]. Additionally, NN control policies have recently received increasing attention in so-called differentiable control (e.g., [12], [13]) and imitation learning for predictive control (e.g., [14], [15]). The interest in NN control policies stems from their scalability for high-dimensional problems and representation capacity due to universal approximation theorem [16]. However, learning NN policies can be sample inefficient, which is especially a challenge in applications where the policy must be learned via interactions with a real system. On the other hand, when a system model is available in the form of differential equations, the model can be used to formulate a continuous-time OCP while a NN policy is leveraged to parameterize the time-varying function of decisions as a state-feedback control policy, allowing for approximating the otherwise intractable OCP. In this approach, path and terminal state constraints can be naturally incorporated into an OCP; what remains a largely open problem in RL.

The solution of a continuous-time OCP with a NN control policy follows the same strategy as learning neural ordinary differential equations (NODEs) [17]. NODEs comprise a class of NN models that replace the discrete nature of hidden layers in dense NNs with a parameterized ODE that represents continuous depth models, effectively describing temporal evolution of the hidden states in inference of dynamics. Such an interpretation of dynamical systems as a learnable function class offers distinct benefits for time-series modeling (e.g., [18], [19]). Specifically, in the realm of continuous-time OCPs, the system dynamics can be viewed as a composition of known (e.g., physics-based) expressions and a NN control policy function embedded in the dynamics, collectively forming a NODE structure [20]. Here, the NN only represents the control policy within a predefined system model, instead of defining the entire set of differential equations as in original NODEs. This setting can be viewed as an instance of the universal differential equation framework [21], which embodies the idea of using various types of NNs within physics-based models. The NODE framework is also applied to the case of unknown dynamics to simultaneously learn and control system dynamics [22], [23].

The dynamic nature of NODEs naturally lends itself to leveraging control-theoretic tools to provide desirable properties such as stability for OCP solutions. There has been a growing body of work on using NNs to learn control Lyapunov functions (CLFs) to establish closed-loop stability properties (e.g., [24]–[26]). Recently, [27] proposed a so-called LyaNet framework for learning NODEs based on the

The authors are with the Department of Chemical and Biomolecular Engineering, University of California, Berkeley, CA 94720, USA. {ipjoshua, gmakr, mesbah}@berkeley.edu

This work was supported by the National Science Foundation under Grant 2130734.

concept of exponentially-stabilizing CLFs [28]. The main idea of LyaNet is to use the supervised loss of the NODE as the potential function, so that the neural network training loss embeds both the learnable dynamics and the potential function, effectively minimizing the so-called Lyapunov loss. For supervised classification via the standard cross entropy loss, [27] shows that not only the learned NODE converges to the equilibrium exponentially fast, i.e., minimizing the NODE inference time, but is also proven to be adversarially robust to uncertainties in initial conditions.

In this work, we present a new approach, termed Lyapunov-NODE control (L-NODEC), for solving continuous-time OCPs for nonlinear systems with known dynamics and constraints and a terminal cost. The objective is to learn a state-feedback neural control policy that stabilizes the system around a desired terminal state. Inspired by [27], we present a Lyapunov loss formulation that embeds an exponentially-stabilizing CLF (ES-CLF) for guaranteeing exponential stability of the controlled system. Additionally, we establish that L-NODEC guarantees adversarial robustness to uncertain initial conditions by deriving an upper bound on the deviation of the terminal states from the target states. We then extend L-NODEC to accommodate system constraints. L-NODEC outperforms baseline NODEC with no stability properties in terms of lower inference times as well as robustness to uncertain initial conditions.

II. PRELIMINARIES

A. Problem Formulation

We consider the continuous-time OCP

$$\min_{\theta} J(x(t_f)) \quad (1a)$$

$$\text{s.t. } \dot{x}(t) = f(x, \pi_{\theta}(x), t), \quad (1b)$$

$$g(x, \pi_{\theta}(x)) \leq 0, \quad (1c)$$

$$\pi_{\theta}(x) \in \mathcal{U}, \quad (1d)$$

$$x(t_0) = x_0, \quad (1e)$$

where $t \in [t_0, t_f]$ is time, $x \in \mathbb{R}^{n_x}$ is the state, $f : \mathbb{R}^{n_x} \times \mathbb{R}^{n_u} \times \mathbb{R} \rightarrow \mathbb{R}^{n_x}$ denotes the known system dynamics, $g_i : \mathbb{R}^{n_x} \times \mathbb{R}^{n_u} \rightarrow \mathbb{R}$ denotes system constraints, and $\pi_{\theta}(x) : \mathbb{R}^{n_x} \rightarrow \mathbb{R}^{n_u}$ is a state-feedback control policy parameterized in terms of parameters $\theta \in \mathbb{R}^{n_{\theta}}$. The control policy is constrained by the compact set $\mathcal{U} \in \mathbb{R}^{n_u}$. The OCP (1) is a particular form of the Bolza problem, known as the Mayer problem [3]. Here, we consider a terminal cost (1a) of the form

$$J(x(t_f)) = \|x(t_f) - x^*\|_2^2, \quad (2)$$

where $\|\cdot\|_2^2$ denotes the l_2 norm and x^* denotes a desired equilibrium point of the system.

The goal is to learn a state-feedback neural control policy $\pi_{\theta}(x(t))$ while ensuring the system is exponentially stable to the equilibrium point x^* and is robust to perturbations in initial conditions x_0 .

B. Neural Ordinary Differential Equations

NODEs provide a useful framework for learning continuous-time ODEs [17]. NODEs can be described by

$$\frac{d\eta}{dt} = h_{\omega}(\eta, u, t), \quad (3)$$

where η denotes the hidden system state at time t , u is the system input, and h_{ω} is a NN parameterized by learnable parameters ω . NODEs are related to the well-known ResNet [29]. The hidden layers in a ResNet architecture can be viewed as a discrete-time Euler approximation to (3); that is, each ResNet layer can be thought of as learning discrete-time dynamics with a fixed time step. For a given input u , (3) can be numerically integrated over a desired time interval to make predictions (i.e., inference). Backpropagation for learning NODEs can be efficiently implemented via the adjoint method [17]. The procedure involves solving a “backward-in-time” ODE, known as the adjoint ODE, associated with (3). Solving the adjoint ODE yields gradients of the loss function with respect to the states η at each time step. These gradients can then be utilized to compute gradients of the loss function with respect to learnable parameters ω using the chain rule [17].

The NODE framework allows for effectively leveraging the well-established numerical solution methods for continuous-time ODEs and NNs to learn continuous-time, data-driven representations for system dynamics. In particular, NODEs enable the use of numerical ODE solvers with a variable time-step, which is especially useful, for example, for inference of stiff system dynamics. Additionally, ODE solvers embedded in NODEs allow for systematic error growth control, as well as trading off numerical accuracy with efficiency. Despite these advantages, the standard NODE framework does not impose desired structures, such as stability or robustness, within the learned dynamics. In particular, lack of stability in NODEs can lead to fragile solutions to (3).

C. Lyapunov Stability

This work looks to enforce stability in learning a NODE model of the form (3) using Lyapunov conditions. Lyapunov theory generalizes the notion of stability of dynamical systems by reasoning about convergence of a system to states that minimize a potential function [30]. Potential functions are a special case of dynamic projection, as defined below.

Definition 1 (Dynamic projection [31]). A continuously differentiable function $V : H \rightarrow \mathbb{R}$ is a dynamic projection if there exist an $\eta^* \in H$ and constants $\underline{\sigma}, \bar{\sigma} > 0$ that satisfy¹

$$\forall \eta \in H : \underline{\sigma} \|\eta - \eta^*\|_2^2 \leq V(\eta) \leq \bar{\sigma} \|\eta - \eta^*\|_2^2. \quad (4)$$

The notion of dynamic projection can be used to define exponential stability as follows.

Definition 2 (Exponential stability). An ODE of the form (3) is exponentially stable if there exist a positive definite dynamic projection potential function V and a constant $\kappa > 0$

¹In principle, Definition 1 holds for any norm, but the l_2 norm is adopted for defining dynamic projection in this work.

such that all solution trajectories of the ODE for all $t \in [t_0, t_f]$ satisfy

$$V(\eta(t)) \leq V(\eta(t_0))e^{-\kappa t}. \quad (5)$$

Here, we use an exponentially stabilizing control Lyapunov function (ES-CLF) to guarantee exponential stability of an ODE of the form (3).

Theorem 1 (Exponentially stabilizing control Lyapunov function [32]). For the ODE (3), a continuously differentiable potential function V is an ES-CLF if there exists a constant $\kappa > 0$ that satisfies

$$\min_{\omega \in \Omega} \left[\frac{\partial V}{\partial \eta} \Big|_{\eta}^{\top} h_{\omega}(\eta, u, t) + \kappa V(\eta) \right] \leq 0 \quad (6)$$

for all $\eta \in H$ and $t \in [t_0, t_f]$. This implies the existence of parameters $\omega \in \Omega$ that yield

$$\frac{\partial V}{\partial \eta} \Big|_{\eta}^{\top} h_{\omega}(\eta, u, t) + \kappa V(\eta) \leq 0. \quad (7)$$

The ODE (3) with parameters ω is exponentially stable with respect to the potential function V and the constant κ . This is also equivalent to the local invariance property [27].

Here, we look to use the NODE framework to determine the state-feedback control policy $\pi_{\theta}(x)$ in the OCP (1) while imposing the ES-CLF structure as specified in (6) and (7). As such, the resulting state-feedback neural control policy will be guaranteed to be exponentially stable with respect to the potential function V .

III. LYAPUNOV-NODE CONTROL (L-NODEC)

In this section, we introduce the proposed Lyapunov-NODE Control (L-NODEC) strategy for learning a state-feedback neural control policy for the OCP (1). By embedding the neural control policy $\pi_{\theta}(x)$ into the known system dynamics (1b), the continuous-time evolution of states of the controlled system is described by

$$x(t) = x(t_0) + \int_{t_0}^t f(x(\tau), \pi_{\theta}(x(\tau)), \tau) d\tau. \quad (8)$$

To learn the neural control policy, we must first define a loss function. This entails defining three components, namely a potential function, pointwise Lyapunov loss, and Lyapunov loss, as discussed below.

For each state dimension i , we denote the state and its desired terminal state by $x_i(t)$ and x_i^* , respectively. Accordingly, we define the potential function as the following weighted l_2 norm

$$V(x(t)) = \|x(t) - x^*\|_{2,w}^2 = \sum_{i=1}^{n_x} w_i (x_i(t) - x_i^*)^2, \quad (9)$$

with weights $w_i > 0$. Note that, unlike the cost function (2), the potential function (9) is defined in terms of the state $x(t)$ and not the terminal state $x(t_f)$. That is, the potential function (9) seeks to penalize the deviation of $x(t)$ from x^* in order to effectively steer the system to the desired equilibrium x^* .

Theorem 2 (Potential function as a dynamic projection). The potential function $V(x(t))$ given in (9) with the initial state $x(t_0)$ is a dynamic projection if it satisfies

$$\|x(t) - x^*\|_{2,w}^2 \leq \|x(t_0) - x^*\|_{2,w}^2 \quad (10)$$

for $x(t) \in \mathbb{R}^{n_x}$ and $t \in [t_0, t_f]$.

Proof: According to Definition 1, $V(x(t))$ is a dynamic projection if

$$\underline{\sigma} \|x(t) - x^*\|_2^2 \leq \sum_{i=1}^{n_x} w_i (x_i(t) - x_i^*)^2 \leq \bar{\sigma} \|x(t) - x^*\|_2^2. \quad (11)$$

There exist finite and positive constants w_{min} and w_{max} within the weights of (9), i.e., the minimum and maximum weights, such that

$$w_{min} \|x(t) - x^*\|_2^2 \leq \sum_{i=1}^{n_x} w_i (x_i(t) - x_i^*)^2 \leq w_{max} \|x(t) - x^*\|_2^2. \quad (12)$$

Eq. (12) implies that the potential function (9) is a dynamic projection since $V(x(t))$ is lower and upper bounded, as stated in Definition 1. ■

By establishing the potential function (9) as a dynamic projection through Theorem 2, we can now utilize (7) to define a pointwise Lyapunov loss $\mathcal{V}(x(t))$ with respect to the states of the controlled system (8). The pointwise Lyapunov loss is defined as violation of the local invariance for the dynamic projection $V(x(t))$. That is,

$$\mathcal{V}(x(t)) = \max \left\{ 0, \frac{\partial V}{\partial x} \Big|_x^{\top} f(x, \pi_{\theta}(x), t) + \kappa V(x(t)) \right\}. \quad (13)$$

Note that the pointwise Lyapunov loss will take on a non-zero value when it violates the local invariance. To derive the Lyapunov loss, we simply integrate the pointwise Lyapunov loss (13), which corresponds to the violation of the local invariance for the entire time domain

$$\mathcal{L}(\theta) = \int_{t_0}^{t_f} \mathcal{V}(x(t)) dt. \quad (14)$$

The proposed L-NODEC strategy uses the Lyapunov loss (14) to learn the state-feedback neural control policy π_{θ} so that the learned policy is guaranteed to yield exponentially stable state trajectories for the controlled system (8). The justification for using the Lyapunov loss (14) for learning π_{θ} stems from the underlying structure of (13), which enforces $\mathcal{V} \geq 0$. This is equivalent to satisfying (6) and (7) according to Theorem 1.

Theorem 3 (Exponential stability of L-NODEC). If there exists θ^* such that $\mathcal{L}(\theta^*) = 0$, then the potential function $V(\theta^*)$ (9) is an ES-CLF according to (7). Accordingly, the controlled system (8) with the state-feedback neural control policy $\pi_{\theta^*}(x)$ will be exponentially stable.

Proof: The proof directly follows from the result of Theorem 1. ■

Furthermore, L-NODEC yields neural control policies that are adversarially robust. This property naturally arises from the pointwise Lyapunov loss (13) with the local invariance property since exponential stability will steer the states to the

desired equilibrium states. To analyze adversarial robustness, we must first define stable inference dynamics.

Definition 3 (δ -Stable inference dynamics for $(x(t_0), x^*)$ [27]). For a dynamical system of the form (8) with a global Lipschitz constant L and a potential function $V(x(t))$, $(x(t_0), x^*)$ has δ -stable inference dynamics if it satisfies:

- 1) Exponential stability: The potential function $V(x(t))$ fulfils the condition specified in (7);
- 2) δ -final loss: The potential function at the final time t_f satisfies $V(x(t_f)) \leq e^{-\kappa t_f} V(x(t_0)) \leq \delta$ for a constant $\kappa > 0$.

In essence, Definition 3 states that the controlled system (8) is exponentially stable, and that the corresponding potential function at the final inference time t_f is bounded by a constant δ . Accordingly, Theorem 3 states if a neural control policy is learned such that $\mathcal{L}(\theta^*) = 0$, then the corresponding potential function (9) will be an ES-CLF with δ -stable inference dynamics according to Definition 3. To analyze adversarial robustness, we establish an upper bound on δ .

Theorem 4 (Adversarial robustness of L-NODEC). For a dynamical system of the form (8) with initial-final state pair $(x(t_0), x^*)$ that satisfies the conditions of Definition 3, a perturbation ϵ to the initial state $x(t_0)$, where $\|\epsilon\|_\infty \leq \bar{\epsilon}$, ensures δ is upper bounded according to

$$\delta \leq \|x(t_0) - x^*\|_{2,w}^2 - \frac{L\bar{\epsilon}}{\kappa}(1 - e^{-\kappa}). \quad (15)$$

Proof: Without loss of generality, $t \in [t_0, t_f]$ is rescaled to $[0, 1]$. We begin by taking the derivative of the potential function $V(x(t))$ with respect to time

$$\dot{V}(x) = \frac{d}{dt}V(x) = \frac{\partial V}{\partial x} \Big|_x^\top f(x, \pi_\theta(x), t). \quad (16)$$

$$\dot{V}(x + \epsilon) \quad (17)$$

$$= \dot{V}(x) + \dot{V}(x + \epsilon) - \dot{V}(x) \quad (18)$$

$$\leq \dot{V}(x) + |\dot{V}(x + \epsilon) - \dot{V}(x)| \quad (19)$$

$$\leq \dot{V}(x) + \left| \frac{\partial V}{\partial x}^\top f(x + \epsilon, \pi_\theta(x + \epsilon), t) \right. \quad (20)$$

$$\left. - \frac{\partial V}{\partial x}^\top f(x, \pi_\theta(x), t) \right|$$

$$\leq \dot{V}(x) + L_V L_f \|\epsilon\|, \quad (21)$$

where in (21) the global uniform Lipschitz property for functions V and f are denoted by L_V and L_f , respectively. We simplify notation by defining $L = L_V L_f$ and apply the adversarial disturbance bound $\|\epsilon\| \leq \bar{\epsilon}$

$$\leq \dot{V}(x) + L\bar{\epsilon} \quad (22)$$

$$\leq -\kappa V(x) + L\bar{\epsilon}. \quad (23)$$

In (23), the result of Theorem 1 is invoked to rewrite the inequality based on exponential stability. We now consider a dynamical system with the upper bound of (23), i.e.,

$$\dot{\gamma} = -\kappa\gamma(t) + L\bar{\epsilon}. \quad (24)$$

Since (24) is a linear ODE, it can be solved for γ

$$\gamma(t) = e^{-\kappa t} c + \frac{L\bar{\epsilon}}{\kappa}, \quad (25)$$

where c is a constant. By specifying the initial condition $\gamma(0)$, (25) can be rewritten as

$$\gamma(t) = e^{-\kappa t} \gamma(0) + \frac{L\bar{\epsilon}}{\kappa}(1 - e^{-\kappa t}). \quad (26)$$

To use the Comparison Lemma [33], we must specify the initial condition $\gamma(0)$ such that $V(x(0)) \leq \gamma(0)$ holds. Recall Definition 3 with the second condition $e^{-\kappa} V(x(0)) \leq \delta$ rescaled to $t \in [0, 1]$, which yields $V(x(0)) \leq \delta e^\kappa$. By choosing $\gamma(0) = \delta e^\kappa$, we obtain

$$\gamma(t) = \delta e^{\kappa(1-t)} + \frac{L\bar{\epsilon}}{\kappa}(1 - e^{-\kappa t}). \quad (27)$$

We now show that the conditions to satisfy the Comparison Lemma are fulfilled as follows: itemsep=3pt

- 1) $\dot{V}(x)$ and $\dot{\gamma}(t)$ are both continuous in state and time;
- 2) $\dot{V}(x) \leq \dot{\gamma}(t)$ for $t \in [0, 1]$ since $\dot{\gamma}(t)$ is the upper bound of $\dot{V}(x)$ as seen in (17) - (24);
- 3) $V(x(0)) \leq \gamma(0)$.

Therefore, it can be concluded that $V(x) \leq \gamma(t)$. Recall it is established in Theorem 2 that

$$V(x) \leq \|x(0) - x^*\|_{2,w}^2.$$

It suffices to show that $\gamma(t) \leq \|x(0) - x^*\|_{2,w}^2$. Accordingly, (27) can be upper bounded at the final time $t = 1$ as

$$\delta + \frac{L\bar{\epsilon}}{\kappa}(1 - e^{-\kappa}) \leq \|x(0) - x^*\|_{2,w}^2, \quad (28)$$

$$\delta \leq \|x(0) - x^*\|_{2,w}^2 - \frac{L\bar{\epsilon}}{\kappa}(1 - e^{-\kappa}). \quad (29)$$

This is equivalent to (15) for the rescaled time $t \in [0, 1]$. ■

The upper bound on δ provides a guarantee on the adversarial robustness of the state-feedback neural control policy learned via L-NODEC. That is, if the dynamics of the controlled system (8) are exponentially stable, the dynamics will also remain exponentially stable with perturbations in the initial conditions $x(t_0)$.

IV. L-NODEC LEARNING FRAMEWORK

The goal of the L-NODEC strategy is to learn a state-feedback neural control policy for the OCP (1) by minimizing the Lyapunov loss (14) for a given initial-final state pair of $(x(t_0), x^*)$. Here, we discuss how system constraints can be incorporated into the learning framework, followed by presenting the L-NODEC algorithm.

A. System constraints

The L-NODEC strategy of Section III can be modified to enforce the state and input constraints (1c) and (1d), respectively, for practical control problems. The system inputs designed by the neural control policy can be constrained in the last layer of the neural policy by using a sigmoid activation function. The sigmoid activation function is commonly defined

as $\phi(\cdot): \mathbb{R} \rightarrow [0, 1]$, but it can be rescaled to the desired bounds with constants u^{lb} and u^{ub} as follows

$$u_i = u_i^{lb} + (u_i^{ub} - u_i^{lb}) \phi(\cdot), \quad (30)$$

for $i \in [1, \dots, n_u]$. To enforce state constraints (1c), penalty terms in the form of quadratic of the constraint violation [34] are appended to the pointwise Lyapunov loss (13), leading to

$$\mathcal{V}_c(x(t)) = \max \left\{ 0, \frac{\partial V}{\partial x} \Big|_x^\top f_\theta(x, \pi_\theta(x), t) + \kappa V(x(t)) \right\} + \sum_i \lambda_i \max \{0, g_i(x, \pi_\theta(x))\}^2, \quad (31)$$

where λ_i is a penalty parameter for each constraint g_i . This is a popular approach to enforcing state constraints since the penalty convergence theorem guarantees a feasible solution to the reformulated unconstrained optimization problem, which is equivalent to solving a constrained optimization problem with Karush-Kuhn-Tucker (KKT) multipliers ([35]–[37]). However, since the pointwise loss (31) is composed of two terms, there will naturally exist a tradeoff between exponential stability of the controlled system (8) and satisfaction of the state constraints (1c), as further discussed in Section V.

B. Neural control policy learning

To learn the neural control policy $\pi_\theta(x)$, the Lyapunov loss function (14) must be discretized. To this end, the time interval $[t_0, t_f]$ can be discretized into Γ uniform segments. This results in a discretized Lyapunov loss as

$$\mathcal{L}(\theta) \approx \sum_{i=0}^{\Gamma-1} \mathcal{V}(x(t_i)), \quad (32)$$

which can be evaluated in terms of the pointwise Lyapunov loss (13), or the constrained pointwise Lyapunov loss (31).

For policy learning, instead of directly backpropagating through the dynamics of the controlled system (8) that can be prohibitively expensive, the adjoint sensitivity method [38] is used to backpropagate through an adjoint ODE

$$a(t) = \frac{\partial \mathcal{L}}{\partial x}, \quad (33)$$

$$\frac{da(t)}{dt} = a(t)^\top \frac{\partial f(x(t), \pi_\theta(x(t)), t)}{\partial x}, \quad (34)$$

where $a(t)$ is the adjoint variable. Equation (34) is solved backwards using an ODE solver with the initial condition $a(t_f)$, along with solving for the dynamics of the controlled states $x(t)$ in (8). This provides the necessary variables to compute the gradient $d\mathcal{L}/d\theta$ for backpropagation [17]

$$\frac{d\mathcal{L}}{d\theta} = - \int_{t_f}^{t_0} a(t)^\top \frac{\partial f(x(t), \pi_\theta(x(t)), t)}{\partial \theta} dt. \quad (35)$$

The L-NODEC algorithm for learning state-feedback neural control policies for the continuous-time OCP (1) is summarized in Algorithm 1. For a given initial-final state pair $(x(t_0), x^*)$, a trajectory of states is generated from iteratively deriving the optimal input with π_θ and using an ODE solver

Algorithm 1 The L-NODEC algorithm for learning state-feedback neural control policies for the continuous-time OCP (1).

```

1: define
2:    $M$  number of max iterations of policy learning
3:    $\Gamma$  number of time discretization segments in (32)
4:    $\alpha$  learning rate
5: define time interval  $t_0, t_1, \dots, t_\Gamma - 1$ 
6: for  $k \leq M$  do
7:   for  $n \leq \Gamma - 1$  do
8:     compute potential  $V(x(t_n))$  via (9)
9:     compute pointwise Lyapunov loss  $\mathcal{V}(x(t_n))$  via (13)
10:    compute  $x(t_{n+1})$  with  $\pi_\theta(x(t_n))$  via (8)
11:   end for
12:   compute Lyapunov loss  $\mathcal{L}(\theta)$  via (32)
13:   update  $\theta \leftarrow \theta - \alpha(d\mathcal{L}(\theta)/d\theta)$  via (35)
14: end for
15: return  $\theta$ 

```

to determine the next state according to (8). This allows for evaluating the potential function (9), the pointwise Lyapunov loss (13) or (31), and the Lyapunov loss (32). The Lyapunov loss is then utilized to update the neural state-feedback control policy π_θ via backpropagation with the adjoint method.

V. CASE STUDIES

The performance of the proposed L-NODEC strategy is demonstrated on a benchmark double integrator problem and a cold atmospheric plasma system with prototypical applications in plasma medicine. The performance of L-NODEC is compared to that of neural ODE control (NODEC) [20].²

A. Double integrator problem

The classic continuous-time double integrator problem [39], modified to a Mayer problem, is defined as

$$\min_{\theta} (x_1(t_f) - 1)^2 \quad (36a)$$

$$\text{s.t. } \dot{x}_1(t) = x_2, \quad (36b)$$

$$\dot{x}_2(t) = u, \quad (36c)$$

$$u = \pi_\theta(x), \quad (36d)$$

$$x_2(t) \leq x_2^{ub}, \quad (36e)$$

where x_1 denotes position (m), x_2 denotes velocity (m/s), $x_2^{ub} = 2.2$ denotes the upper constraint for x_2 , and π_θ denotes the neural control policy parameterized by 3 hidden layers of 32 nodes each. The initial state $x(t_0)$ is set to $(0, 0)$. We consider two cases: unconstrained L-NODEC with $t_f = 1.5$ s wherein the state constraint (36e) is ignored and constrained L-NODEC that solves the OCP (36) with $t_f = 2.0$ s. In both cases, the potential function is defined according to (9) with $w_1 = 1$ and $w_2 = 10^{-4}$.

²The codes for the implementation of the LNODEC strategy can be found at <https://github.com/ipjoshua1483/LNODEC>

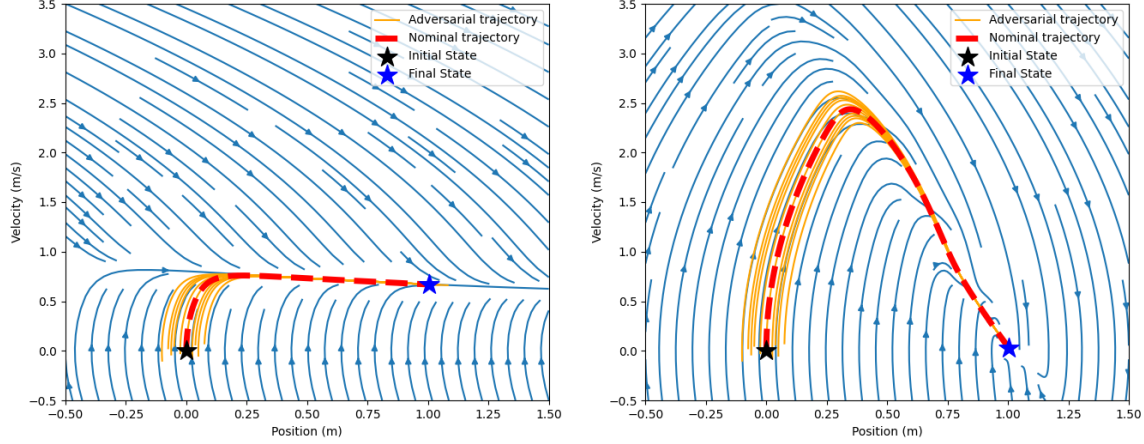


Fig. 1. Phase portraits of the controlled double integrator system. Left: State trajectories for NODEC. Right: State trajectories for L-NODEC. Blue trajectories signify streamlines in the phase space. The nominal trajectory is shown in red and the adversarial trajectories with respect to perturbations in initial states are shown in orange.

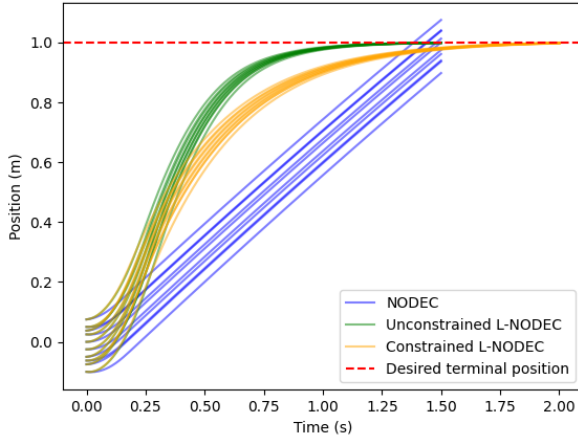


Fig. 2. Position trajectories of the double integrator system controlled using the state-feedback neural control policies designed by NODEC, unconstrained L-NODEC, and constrained L-NODEC for 10 adversarial perturbations in the initial states. Note that the terminal time for NODEC and unconstrained L-NODEC is $t_f = 1.5$ s, whereas for constrained L-NODEC is $t_f = 2.0$ s.

Fig. 1 shows the phase portrait of the state trajectories for unconstrained L-NODEC, as compared to NODEC that does not impose the proposed Lyapunov condition in learning the neural control policy. Trajectories corresponding to perturbations in the initial state are also displayed. It is observed that the L-NODEC trajectories reach the final state with zero velocity, meaning the controlled system is in equilibrium with the environment. On the other hand, the NODEC strategy cannot steer the controlled system to the equilibrium since it is not explicitly informed of it through the Lyapunov loss function (14); hence, the terminal velocity is non-zero.

We first observe differences in the nominal trajectories for the L-NODEC and NODEC strategies. In L-NODEC, the peak velocity is significantly greater, which allows the position to

change greatly in a short time. However, it is also capable of reducing its velocity to terminate at zero velocity at the final time and achieve equilibrium, unlike the NODEC case. Furthermore, the L-NODEC strategy is adversarially robust as it allows perturbations from the nominal initial condition to still reach the desired terminal equilibrium state. This is because of the exponential stability of the L-NODEC policy, which will also provide the same stability for the perturbed initial states around a radius of the original initial condition. This is while NODEC does not have any stability guarantees incorporated in its formation and, thus, performs poorly under perturbations in initial conditions, as evidenced by the adversarial trajectories not terminating at the target position (see Fig. 1 left).

Fig. 2 shows the position trajectories of the double integrator controlled using the neural control policies designed by NODEC, unconstrained L-NODEC, and constrained L-NODEC. As discussed above, L-NODEC enforces stability around the terminal equilibrium with zero terminal velocity unlike NODEC, which is also observed in Fig. 2. Further, L-NODEC exhibits superior performance throughout $[t_0, t_f]$, as it yields positions that have lower l_2 distance to the desired terminal position. It is also evident that L-NODEC provides more adversarial robustness since the 10 adversarial trajectories reach the terminal position at t_f , whereas the NODEC trajectories do not. Fig. 2 also suggests that the constrained L-NODEC strategy reaches the desired terminal position, but requires a longer time. This is expected due to the tradeoff between the exponential stability condition and constraint satisfaction, as seen in the loss (31).

Fig. 3 shows the time-evolution of the potential function $V(x(t))$ for unconstrained and constrained L-NODEC, along with the exponential stability threshold from (5) as a baseline. As can be seen, the learned neural control policies are capable of steering the system to below the exponential stability threshold within $[t_0, t_f]$. This is while the the constrained L-NODEC strategy yields trajectories that require more time to meet the exponential stability threshold due to the tradeoff

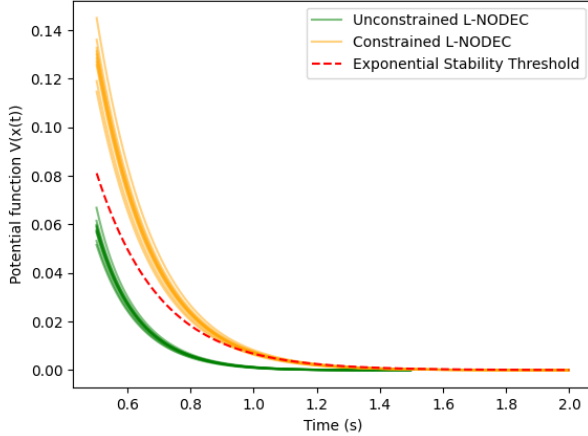


Fig. 3. Time-evolution of the normalized potential function for the double integrator system controlled by the state-feedback neural control policies designed by L-NODEC in the absence and presence of the state constraint.

between exponential stability and constraint satisfaction.

B. Control of thermal dose delivery using a cold atmospheric plasma biomedical system

Cold atmospheric plasmas (CAPs) are used for treatment of heat- and pressure-sensitive biomaterials in a wide range of applications, including plasma medicine [40]. Atmospheric pressure plasma jets (APPJs) are the most commonly used CAP discharge type in biomedical applications [40], yet safe, reproducible and therapeutically effective control of APPJs is particularly challenging [41]–[43]. Here, we focus on optimal control of the nonlinear and cumulative thermal effects of APPJs on a target surface. The control objective is to deliver a desired amount of thermal dose, quantified in terms of cumulative equivalent minutes (CEM) [44], to a surface within a prespecified treatment time while maintaining the surface temperature below a safety-critical threshold. The OCP is formulated as [45]

$$\min_{\theta} (x_2(t_f) - 1.5)^2 \quad (37a)$$

$$\text{s.t. } \dot{x}_1(t) = \frac{u}{3.1981} - \frac{0.8088}{\ln(x_1(t) - 25) - \ln(x_1(t) - 35)}, \quad (37b)$$

$$\dot{x}_2(t) = \frac{0.5^{(43-x_1(t))}}{60}, \quad (37c)$$

$$u = \pi_{\theta}(x), \quad (37d)$$

$$x_1(t) \leq x_1^{ub}, \quad (37e)$$

where x_1 denotes the surface temperature ($^{\circ}\text{C}$), x_2 denotes the thermal dose CEM (min) with the desired terminal value of 1.5 min, $x_1^{ub} = 45^{\circ}\text{C}$ is the surface temperature threshold, the control input u is the power applied to CAP (W), and $t_f = 100$ s is the treatment time. The CAP treatment starts from the initial condition $x(t_0) = (37, 0)$. Similar to the double integrator problem, we set $w_1 = 1$ and $w_2 = 10^{-4}$ in the

potential function (9). The policy π_{θ} is set to 3 hidden layers of 32 nodes each.

We compare the performance of L-NODEC to that of NODEC in learning the state-feedback neural control policy $\pi_{\theta}(x)$ in (37). Fig. 4 shows the CEM delivered to the target surface, surface temperature, and a sample control input of the applied power for each strategy. The training of the neural control policy is repeated 20 times for each strategy to evaluate the variability in the learned control policies and, thus, the resulting state profiles. The state trajectories are truncated when the desired terminal thermal dose is reached to avoid the delivery of excessive thermal dose to the target surface. The L-NODEC policies consistently increase the temperature in the initial phase of the CAP treatment till it reaches the temperature constraint. As a result, the corresponding thermal dose CEM reaches the desired terminal CEM of 1.5 min in less than 60 s, whereas NODEC policies require the entire treatment time of 100 s to realize the terminal CEM target. This is a particularly significant result in the context of plasma medicine since shorter treatment times are highly desirable because of patient safety and comfort [43]. Furthermore, NODEC policies lead to state trajectories with much larger variability and several temperature constraint violations. The latter can be attributed to the vastly different nature of the learned control policies, as shown in Fig. 4(c). The L-NODEC policy initially maintains the applied power at a higher level, which allows for quicker accumulation of CEM. Then, it reduces the applied power level once it is close to reaching the terminal CEM target. On the other hand, the NODEC policy maintains a lower level of applied power to gradually accumulate CEM. This results in profound differences in the CEM and surface temperature profiles, as discussed above.

VI. CONCLUSION

This paper presented a method for learning state-feedback neural control policies for continuous-time optimal control problems with a terminal cost using the notion of neural ordinary differential equations. The exponential stability and adversarial robustness of the proposed method are established. The key advantages of the method include ensuring stability of the controlled system and enabling lower inference times in steering a system to its desired terminal state. The method is extended to account for system constraints. Future work will investigate alternative approaches to constraint handling beyond the soft quadratic penalty function.

REFERENCES

- [1] M. Athans and P. L. Falb, *Optimal control: an introduction to the theory and its applications*. Courier Corporation, 2007.
- [2] F. L. Lewis, D. Vrabie, and V. L. Syrmos, *Optimal control*. John Wiley & Sons, 2012.
- [3] A. E. Bryson, *Applied optimal control: optimization, estimation and control*. Routledge, 2018.
- [4] K.-L. Teo, C.-J. Goh, K.-H. Wong *et al.*, *A unified computational approach to optimal control problems*. Longman Scientific & Technical New York, 1991, vol. 113.
- [5] L. T. Biegler, A. M. Cervantes, and A. Wächter, “Advances in simultaneous strategies for dynamic process optimization,” *Chemical Engineering Science*, vol. 57, no. 4, pp. 575–593, 2002.

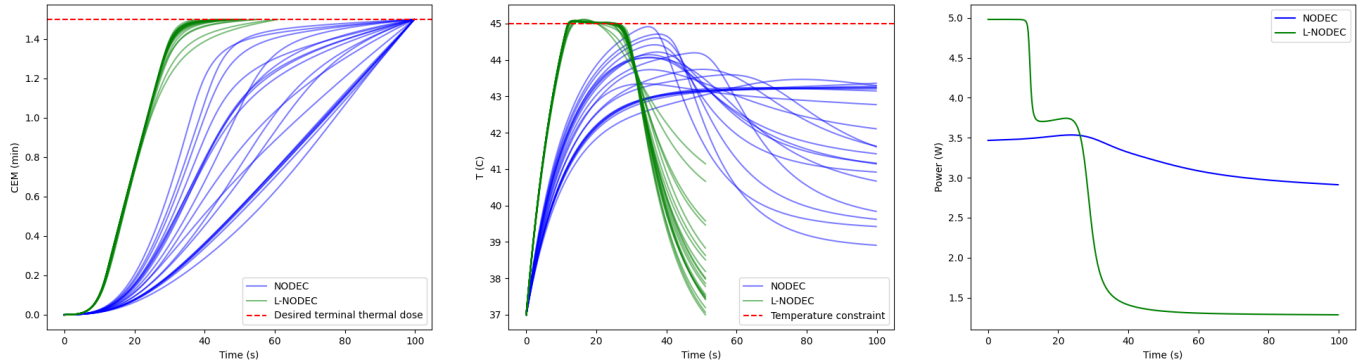


Fig. 4. Optimal control of thermal dose delivery of cold atmospheric plasma to a target surface. (a) The delivered thermal dose CEM. (b) Surface temperature. (c) A sample control input, i.e., applied power to plasma, designed by NODEC and L-NODEC. 20 state profiles are shown based on repeated training of the state-feedback neural control policy for each strategy. Note that the plasma treatment is terminated once the desired terminal thermal dose is reached and, thus, the trajectories are truncated when CEM reaches 1.5 min.

- [6] R. F. Hartl, S. P. Sethi, and R. G. Vickson, "A survey of the maximum principles for optimal control problems with state constraints," *SIAM Review*, vol. 37, no. 2, pp. 181–218, 1995.
- [7] R. Luus, *Iterative dynamic programming*. Chapman and Hall, 2019.
- [8] B. Chachuat, A. B. Singer, and P. I. Barton, "Global methods for dynamic optimization and mixed-integer dynamic optimization," *Industrial & Engineering Chemistry Research*, vol. 45, pp. 8373–8392, 2006.
- [9] D. Rodrigues and A. Mesbah, "Efficient global solutions to single-input optimal control problems via approximation by sum-of-squares polynomials," *IEEE Transactions on Automatic Control*, vol. 67, no. 9, pp. 4674–4686, 2022.
- [10] R. S. Sutton and A. G. Barto, *Reinforcement Learning: An Introduction*. MIT Press, Cambridge, 2018.
- [11] D. Bertsekas, *Reinforcement learning and optimal control*. Athena Scientific, 2019, vol. 1.
- [12] W. Jin, Z. Wang, Z. Yang, and S. Mou, "Pontryagin differentiable programming: An end-to-end learning and control framework," *Advances in Neural Information Processing Systems*, vol. 33, pp. 7979–7992, 2020.
- [13] J. Drgoňa, K. Kiš, A. Tuor, D. Vrabie, and M. Klaučo, "Differentiable predictive control: Deep learning alternative to explicit model predictive control for unknown nonlinear systems," *Journal of Process Control*, vol. 116, pp. 80–92, 2022.
- [14] B. Karg and S. Lucia, "Efficient representation and approximation of model predictive control laws via deep learning," *IEEE Transactions on Cybernetics*, vol. 50, no. 9, pp. 3866–3878, 2020.
- [15] J. A. Paulson and A. Mesbah, "Approximate closed-loop robust model predictive control with guaranteed stability and constraint satisfaction," *IEEE Control Systems Letters*, vol. 4, no. 3, pp. 719–724, 2020.
- [16] A. R. Barron, "Universal approximation bounds for superpositions of a sigmoidal function," *IEEE Transactions on Information Theory*, vol. 39, no. 3, pp. 930–945, 1993.
- [17] R. T. Chen, Y. Rubanova, J. Bettencourt, and D. K. Duvenaud, "Neural ordinary differential equations," *Advances in neural information processing systems*, vol. 31, 2018.
- [18] A. Rahman, J. Drgoňa, A. Tuor, and J. Strube, "Neural ordinary differential equations for nonlinear system identification," in *Proceedings of the American Control Conference*, 2022, pp. 3979–3984.
- [19] A. J. Linot, J. W. Burby, Q. Tang, P. Balaprakash, M. D. Graham, and R. Maulik, "Stabilized neural ordinary differential equations for long-time forecasting of dynamical systems," *Journal of Computational Physics*, vol. 474, p. 111838, 2023.
- [20] I. O. Sandoval, P. Petsagkourakis, and E. A. del Rio-Chanona, "Neural odes as feedback policies for nonlinear optimal control," *IFAC-PapersOnLine*, vol. 56, no. 2, pp. 4816–4821, 2023.
- [21] C. Rackauckas, Y. Ma, J. Martensen, C. Warner, K. Zubov, R. Supekar, D. Skinner, A. Ramadhan, and A. Edelman, "Universal differential equations for scientific machine learning," *arXiv:2001.04385*, 2020.
- [22] S. Bachhuber, I. Weygers, and T. Seel, "Neural ODEs for data-driven automatic self-design of finite-time output feedback control for unknown nonlinear dynamics," *IEEE Control Systems Letters*, 2023.
- [23] C. Chi, "Nodec: Neural ode for optimal control of unknown dynamical systems," *arXiv preprint arXiv:2401.01836*, 2024.
- [24] Y.-C. Chang, N. Roohi, and S. Gao, "Neural Lyapunov control," *Advances in Neural Information Processing Systems*, vol. 32, 2019.
- [25] S. Mukherjee, J. Drgoňa, A. Tuor, M. Halappanavar, and D. Vrabie, "Neural Lyapunov differentiable predictive control," in *Proceedings of the 61st IEEE Conference on Decision and Control*, 2022, p. 2097.
- [26] L. Zhao, K. Miao, K. Gatsis, and A. Papachristodoulou, "NLBAC: A neural ordinary differential equations-based framework for stable and safe reinforcement learning," *arXiv preprint arXiv:2401.13148*, 2024.
- [27] I. D. J. Rodriguez, A. D. Ames, and Y. Yue, "LyaNet: A Lyapunov Framework for Training Neural ODEs," 2022.
- [28] A. D. Ames, K. Galloway, K. Sreenath, and J. W. Grizzle, "Rapidly exponentially stabilizing control Lyapunov functions and hybrid zero dynamics," *IEEE Transactions on Automatic Control*, vol. 59, p. 876, 2014.
- [29] E. Haber and L. Ruthotto, "Stable architectures for deep neural networks," *Inverse Problems*, vol. 34, no. 1, p. 014004, 2017.
- [30] J. L. Salle and S. Lefschetz, *Stability by Liapunov's Direct Method: With Applications*. New York: Academic Press, 1961.
- [31] A. J. Taylor, V. D. Dorobantu, M. Krishnamoorthy, H. M. Le, Y. Yue, and A. D. Ames, "A control Lyapunov perspective on episodic learning via projection to state stability," in *Proceedings of the 58th IEEE Conference on Decision and Control*, 2019.
- [32] A. D. Ames, K. Galloway, K. Sreenath, and J. W. Grizzle, "Rapidly exponentially stabilizing control Lyapunov functions and hybrid zero dynamics," *IEEE Transactions on Automatic Control*, vol. 59, no. 4, pp. 876–891, 2014.
- [33] H. K. Khalil, *Nonlinear systems; 3rd ed.* Upper Saddle River, NJ: Prentice-Hall, 2002, the book can be consulted by contacting: PH-AID: Wallet, Lionel. [Online]. Available: <https://cds.cern.ch/record/1173048>
- [34] D. P. Bertsekas, "Necessary and sufficient conditions for a penalty method to be exact," *Mathematical programming*, vol. 9, pp. 87–99, 1975.
- [35] R. M. Freund, "Penalty and barrier methods for constrained optimization," 2004.
- [36] X. Chen, Z. Lu, and T. K. Pong, "Penalty methods for a class of non-lipschitz optimization problems," *SIAM Journal on Optimization*, vol. 26, no. 3, pp. 1465–1492, 2016.
- [37] G. Di Pillo, *Exact Penalty Methods*. Dordrecht: Springer Netherlands, 1994, pp. 209–253.
- [38] L. S. Pontryagin, E. F. Mishchenko, V. G. Boltyanskii, and R. V. Gamkrelidze, *The Mathematical Theory of Optimal Processes*, 1962.
- [39] J. Logsdon and L. Biegler, "Decomposition strategies for large-scale dynamic optimization problems," *Chemical Engineering Science*, vol. 47, pp. 851–864, 1992.
- [40] M. Laroussi, S. Bekechus, M. Keidar, A. Bogaerts, A. Fridman, X. Lu, K. Ostrikov, M. Hori, K. Stapelmann, V. Miller *et al.*, "Low-temperature plasma for biology, hygiene, and medicine: Perspective and roadmap," *IEEE Transactions on Radiation and Plasma Medical Sciences*, vol. 6, no. 2, pp. 127–157, 2021.
- [41] D. Gidon, D. B. Graves, and A. Mesbah, "Effective dose delivery in atmospheric pressure plasma jets for plasma medicine: A model

- predictive control approach,” *Plasma Sources Science and Technology*, vol. 26, no. 8, p. 085005, 2017.
- [42] —, “Predictive control of 2d spatial thermal dose delivery in atmospheric pressure plasma jets,” *Plasma Sources Science and Technology*, vol. 28, no. 8, p. 085001, 2019.
- [43] A. D. Bonzanini, K. Shao, A. Stancampiano, D. B. Graves, and A. Mesbah, “Perspectives on machine learning-assisted plasma medicine: Toward automated plasma treatment,” *IEEE Transactions on Radiation and Plasma Medical Sciences*, vol. 6, no. 1, pp. 16–32, 2021.
- [44] S. A. Sapareto and W. C. Dewey, “Thermal dose determination in cancer therapy,” *International Journal of Radiation Oncology*Biophysics*, vol. 10, no. 6, pp. 787–800, 1984.
- [45] D. Rodrigues, K. J. Chan, and A. Mesbah, “Data-driven adaptive optimal control under model uncertainty: An application to cold atmospheric plasmas,” *IEEE Transactions on Control Systems Technology*, vol. 31, no. 1, pp. 55–69, 2023.